Supporting Information
for

Spin crossover in 3d metal centers binding halide-containing ligands: magnetism, structure and computational studies

Paulo N. Martinho,[a] Frederico F. Martins,[a] Nuno A. G. Bandeira,[a] Maria José Calhorda[a]

[a]Centro de Química e Bioquímica and BioISI - Biosystems & Integrative Sciences Institute, Faculdade de Ciências, Universidade de Lisboa, Campo Grande, 1749-016 Lisboa, Portugal

Contents

Table S2. Dataset for the correlation analysis displayed in Figures 20-21 of main text.

Ion	Ligands	ΔE_{HS-LS} (kcal mol^{-1})	$\Delta E_{MECP-HS}$ (kcalmol^{-1})	$\Delta E_{MECP-LS}$ (kcal mol^{-1})
Mn(III) d^4	L1 (X=Br)	2.9	47.0	49.9
	L2 (X=Cl)	-10.6	9.6	-1.0
	L2 (X=Br)	0.2	2.2	2.4
	L2 (X=Br)	26.1	6.3	32.3
	L2 (X=Br)	14.2	8.6	22.8
	L2 (X=Br)	39.2	-31.9	7.2
	L1 (X=Cl)	-17.9	81.4	63.5
Fe(III) d^5	L8, L12 (X=F)	5.6	9.7	15.3
	L8, L12 (X=Cl)	5.9	6.8	12.7
	L8, L12 (X=Br)	4.4	3.4	7.8
	L8, L12 (X=I)	3.8	8.2	11.9
	L20(N_3^-) X=Br)	3.4	6.7	10.1
	L20(SC**N**$^-$) (X=Br)	3.8	6.6	10.5
	L20(**Cl**$^-$) (X=Br)	0.4	7.5	7.9
	L20(**N**CSe$^-$) (X=Br)	4.5	6.6	11.2
Fe(II) d^6	L30 (X=Cl)	-0.7	13.5	12.8
	L12 (X=Cl)	2.2	8.0	10.3
	L56 (X=Br)	21.7	1.1	22.7
	L30 (X=I)	8.8	0.2	9.1
	$(L39)_2$(**N**$CS^-)_2$	2.6	4.5	7.1
	$(L40)_2$(**N**$CS^-)_2$	-5.5	8.8	3.3
	L50(C_2**N**$_3^-)_2$	-11.0	17.7	6.7
	L50(C_2**N**$_3^-)_2$	2.3	8.1	10.3
	L12 (X=Cl)	26.4	-16.0	10.4
	L12 (X=Br)	7.8	3.6	11.4
	L12 (X=I)	2.3	5.2	7.5
Co(II) d^7	L56 (X=Br)	-0.3	3.8	3.5

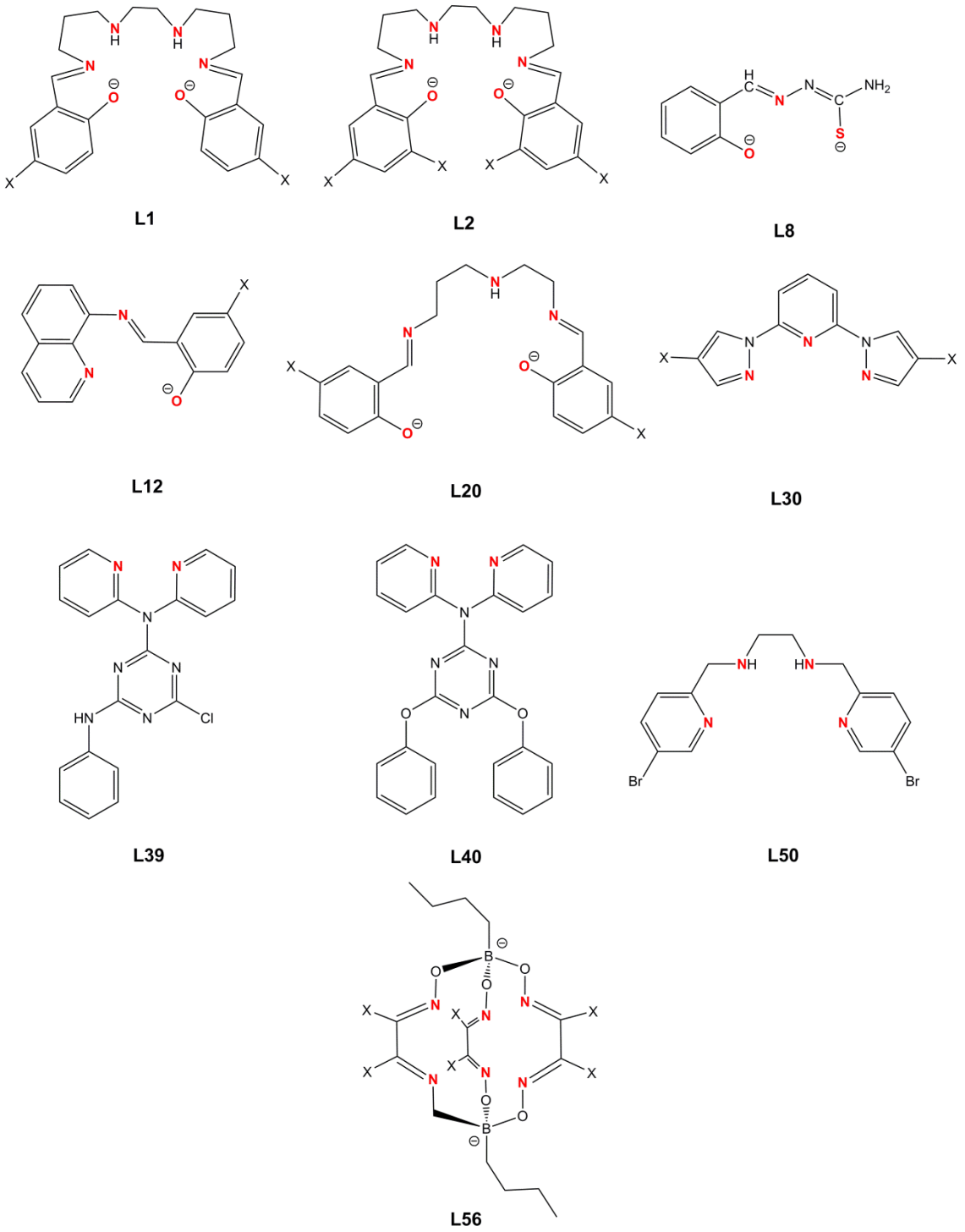

Figure S2. A representation of the ligands presented in Table S1.

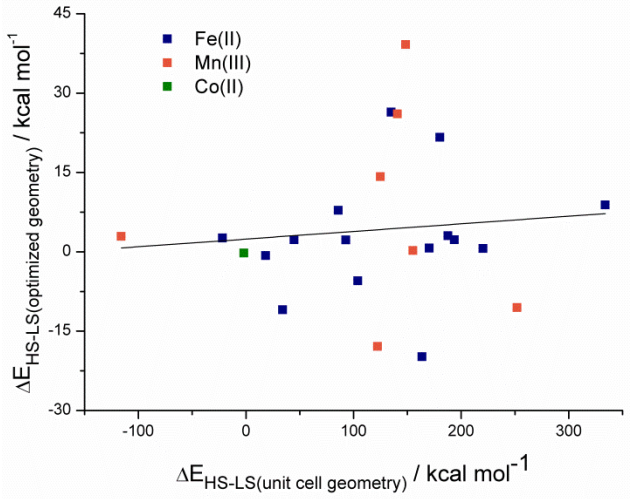

Figure S2. Energy difference calculated between the optimized structures of HS and LS states against the same energy difference between the crystal structures for both spin states (single point calculation) for Fe(II), Mn(III), and Co(II) complexes.

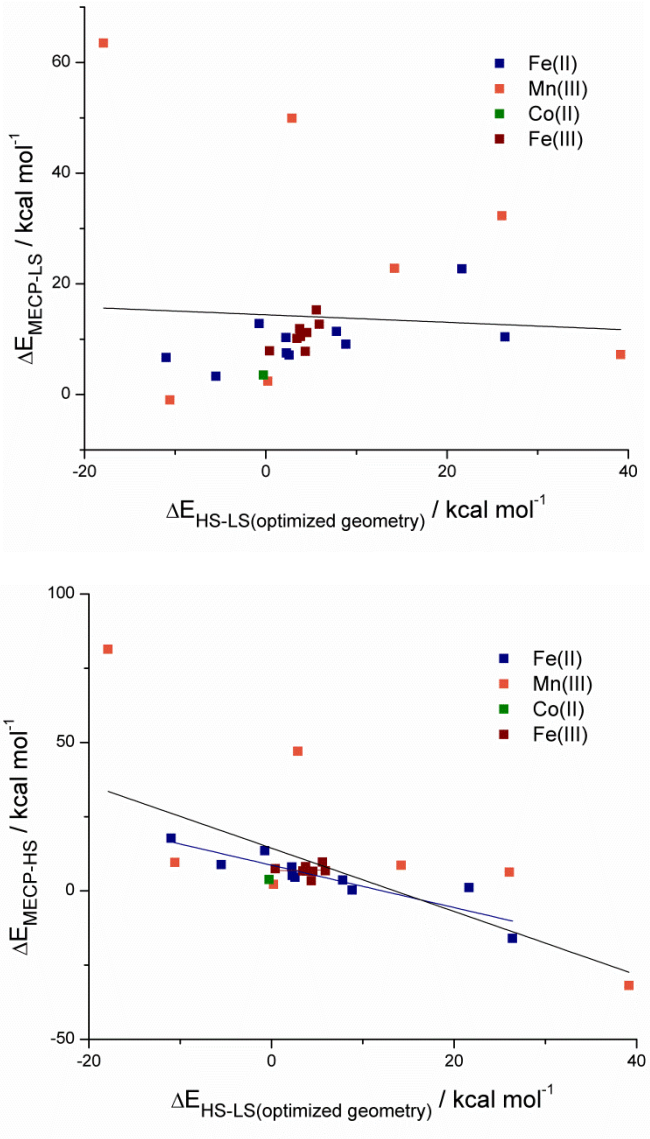

Figure S3. Energy difference between the MECP and the LS (top) or HS (bottom) energy against the energy difference between the HS and LS optimized structures.